**TELKOMNIKA Telecommunication, Computing, Electronics and Control**
Vol. 19, No. 1, February 2021, pp. 192∼198
ISSN: 1693-6930, accredited First Grade by Kemenristekdikti, No: 21/E/KPT/2018
DOI: 10.12928/TELKOMNIKA.v19i1.16245 

# Enabling full-duplex in multiple access technique for 5G wireless networks over Rician fading channels

**Chi-Bao Le[1], Dinh-Thuan Do[2]**
[1]Faculty of Electronics Technology, Industrial University of Ho Chi Minh City (IUH), Vietnam
[2]Wireless Communications Research Group, Faculty of Electrical and Electronics Engineering,
Ton Duc Thang University, Ho Chi Minh City, Vietnam

**Article Info**

***Article history:***

Received Apr 4, 2020
Revised Jul 6, 2020
Accepted Sep 24, 2020

***Keywords:***

Full-duplex
Non-orthogonal multiple access
Outage probability
Unmanned aerial vehicle

**ABSTRACT**

Nowadays, unmanned aerial vehicle (UAV) relays' assisted internet of things (IoT) systems provide facility in order to overcome the large scale fading between source and sink. The full-duplex scheme enables wireless network to provide higher spectrum efficient technology. This paper analyses performance of two users which are served by new emerging non-orthogonal multiple access (NOMA) technique. Exact outage probability of such two users are derived and checked via Monte-Carlo simulation. These analytical results provide guideline to design UAV in real application. This paper provides a comprehensive study to examine impact of interference, fixed power allocation factors to system performance.



***Corresponding Author:***

Dinh-Thuan Do
Wireless Communications Research Group
Faculty of Electrical & Electronics Engineering
Ton Duc Thang University
Ho Chi Minh City, Vietnam
Email: dodinhthuan@tdtu.edu.vn

## 1. INTRODUCTION

State of the art, wireless network provides ability to serve massive connections and such requirement satisfied by the application of non-orthogonal multiple access (NOMA) in fifth generation (5G) networks. NOMA has drawn wide attention due to its potential to improve spectral efficiency [1] and more reliable improvement with relaying scheme [2]. Different from conventional orthogonal multiple access (OMA), NOMA benefits from relaying design, far user can be served by the base station under help of the relay. NOMA enables various applications to serve multiple users to be served at the same time and frequency by superimposing multiple users in the power domain at the transmitter and using successive interference cancellation (SIC) at the receiver [3, 4]. In NOMA system, device-to-device transmission mode is activated based on the users divided into different kinds of categories according to their channel conditions, i.e., the near user and the far user [5].

In the context of NOMA, cooperative mode is mainly divided into two cases. These cases exhibit implementation of NOMA to imrpove performance of users located edge of cell [6–9]. In cooperative NOMA, the near users with strong channel conditions needs to act as relays. The relay provides improved performance of the far users who have poor channel conditions [9, 10]. However. However, half-duplex (HD) mode is studied in the cooperative NOMA relay in the early works [7–11]. The authors in [6] considered full-duplex (FD) relay into cooperative NOMA. The main advantages are reducing delay caused by the dedicated relay

and enhancing end to end transmission quality. The authors in [12] investigated advantage achieved by FD mode, which proved enhancing performance gain. While the authors in [13] maximized energy efficiency for full-duplex cooperative NOMA with power allocation. However, open problem still exists related to fading model. This paper fulfills a gap in [13–22], in which UAV-based relay is not considered.

## 2. SYSTEM MODEL

This paper considers a two-user NOMA architecture, where UE-1 directly exchanges data with the base station (BS) as depicted in Figure 1, while UE-2 receives signals from the BS via unmanned aerial vehicle (UAV) relay. The link BS to UE-2 is supported by a dedicated relay. Note that each node is equipped single antenna except for relay which requires two antenna to provide ability of FD. The probabilistic LoS and non-LoS (NLoS) model for UAV is adopted to indicate the large scale fading. We use such model for the channel between the UAV and terrestrial user due to impact of the density of buildings and the distance between the UAV and users. The probability of user which has benefit of a LoS link is expressed as [24]

$$P_{LoS,k} = \frac{1}{1+pe^{-q(\theta_k - p)}} \quad , k \in \{1,2\} \tag{1}$$

in which we denote $p$ and $q$ are constant values depending on the surrounding environment (sub-urban, urban, dense-urban). Therefore, $\theta_k$ in (1) can be expressed as

$$\theta_k = \arcsin\left(\frac{H}{d_k}\right), \tag{2}$$

in which $H$ denotes the height of UAV, $d_k = \sqrt{r_k^2 + H^2}$ is the distance between user $k$ and the UAV, and $r_k$ is the distance between users and UAV. Obviously, the probability of NLoS is $P_{NLoS,k} = 1 - P_{LoS,k}$.

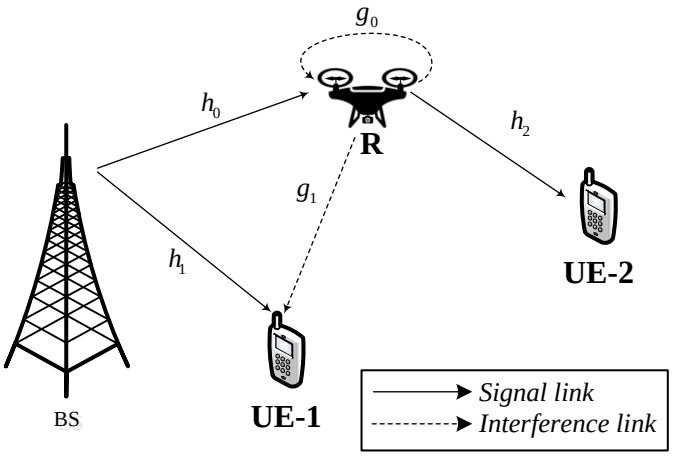


Figure 1. Enabling FD mode in relaying network

The received signal at the relay is expressed by

$$y_R = h_0 \sum_{k=1}^{2} \sqrt{d_S^{-\alpha} \varphi_k P_S} s_k + \sqrt{\kappa P_R} g_0 s_{LI-0} + n_R, \tag{3}$$

where $\kappa$, $0 \leq \kappa \leq 1$ denotes as level of self-interference (LI), $\varphi_k, k = 1, 2$ are power allocation factors to two NOMA users who need receive signal $s_k$, $P_S$ is transmit power of the BS,$s_{LI}$ is self-interference signal due to FD mode, $d_S = \sqrt{r_S^2 + H^2}$ is the distance between $BS$ and UAV, and $\alpha$ is the path loss exponent from the $BS$ to UAV. The signal to interference plus noise (SINR) to detect signal $s_2$ is given by

$$\Gamma_R^{s_2} = \frac{\varphi_2 \rho d_S^{-\alpha} |h_0|^2}{\varphi_1 \rho d_S^{-\alpha} |h_0|^2 + \rho\kappa |g_0|^2 + 1}, \tag{4}$$

where $\rho = P_S/N_0 = P_R/N_0$ is the transmit signal-to-noise radio (SNR). Employing SIC, interference $s_2$ is deleted to detect $s_1$ corresponding SINR as

$$\Gamma_R^{s_1} = \frac{\varphi_1 \rho d_S^{-\alpha} |h_0|^2}{\rho\kappa |g_0|^2 + 1}. \tag{5}$$

Then, the received signal at user UE-1 is given as

$$y_{UE_1} = h_1 \sum_{k=1}^{2} \sqrt{\bar{d}_1^{-\alpha} \varphi_k P_S} \bar{s}_k + \sqrt{P L_1 d_1^{-\alpha} P_R} g_1 s_{LI-1} + n_{UE_1} \tag{6}$$

where $\bar{d}_1$ is the distance between BS to UE-1, $PL_k = (P_{LoS,k} + \upsilon P_{NLoS,k})$, $k \in \{1, 2\}$ and $\upsilon$ denotes the additional attenuation factor of NLoS transmission. The SINR to detect $s_2$ and then $s_1$ at UE-1 are respectively expressed by

$$\Gamma_{UE_1}^{\bar{s}_2} = \frac{\bar{d}_1^{-\alpha} \varphi_2 \rho |h_1|^2}{\bar{d}_1^{-\alpha} \varphi_1 \rho |h_1|^2 + \rho P L_1 d_1^{-\alpha} \kappa |g_1|^2 + 1}, \tag{7a}$$

$$\Gamma_{UE_1}^{\bar{s}_1} = \frac{\varphi_1 \rho \bar{d}_1^{-\alpha} |h_1|^2}{\rho\kappa P L_1 d_1^{-\alpha} |g_1|^2 + 1}. \tag{7b}$$

The received signal and SNR at user UE-2 is formulated respectively as

$$\tilde{y}_{UE_2} = h_2 \sqrt{P L_2 d_2^{-\alpha} P_R} \tilde{s}_2 + n_{UE_2}. \tag{8}$$

$$\Gamma_{UE_2}^{\tilde{s}_2} = \rho P L_2 d_2^{-\alpha} |h_2|^2. \tag{9}$$

## 3. OUTAGE PROBABILITY ANALYSIS

Case 1: $0 < \kappa < 1$, the outage probability without interference link of UE-1 is given by

$$\begin{aligned} \mathcal{OP}_{UE_1} =& 1 - \Pr\left(\Gamma_{UE_1}^{\bar{s}_2} > \varepsilon_2 \cap \Gamma_{UE_1}^{\bar{s}_1} > \varepsilon_1\right) \\ =& 1 - \Pr\left(|h_1|^2 > \bar{\theta}\left(\Delta |g_1|^2 + 1\right)\right), \end{aligned} \tag{10}$$

where $\Delta = \rho P L_1 d_1^{-\alpha} \kappa$, $\bar{\theta} = \max\left(\frac{\bar{\varepsilon}_2}{\rho(\varphi_2 - \varphi_1 \bar{\varepsilon}_2)}, \frac{\bar{\varepsilon}_1}{\varphi_1 \rho}\right)$, $\bar{\varepsilon}_1 = 2^{2R_1} - 1$ with $R_1$ is denoted as the target rate at UE-1 to detect $\bar{s}_1$ and $\bar{\varepsilon}_2 = 2^{2R_2} - 1$ with $R_2$ being the target rate at UE-2 to detect $\bar{s}_2$. Thus, the probability distribution function (PDF) of the unordered squared channel gain $X$, $X \in \{h_0, h_1, h_2, g_0, g_1\}$, is formulated by a non-central chi-square distribution with two degrees of freedom as [25]

$$f_{|X|^2}(x) = \frac{(1 + K_X) e^{-K_X - \frac{(1+K_X)x}{\Omega_X}}}{\Omega_X} \mathcal{I}_0\left(2\sqrt{\frac{K_X (1 + K_X) x}{\Omega_X}}\right), \tag{11}$$

where $\mathcal{I}_0(.)$ is the zeroth-order modified Bessel function of the first kind, $K_X = \frac{|\mu_X|^2}{2\sigma^2}$ is the Rician factor and $\Omega_X = \mathbb{E}\left\{|X|^2\right\} = 1$ is the normalized average fading power. The corresponding cumulative distribution function (CDF) is known as

$$F_{|X|^2}(x) = 1 - \mathcal{Q}\left(\sqrt{2K_X}, \sqrt{\frac{2(1 + K_X) x}{\Omega_X}}\right), \tag{12}$$

where $\mathcal{Q}(\nu, \iota) \triangleq \int_\iota^\infty x e^{-\frac{\nu^2 + x^2}{2}} \mathcal{I}_0(ax)$ denotes the MarcumQ-function of first order. By using result included in [23, Eq. (8.445)] with $\mathcal{I}_0(z) = \sum_{r=0}^{\infty} \frac{z^{2r}}{r!\Gamma(r+1)2^{2r}}$, the $\mathcal{OP}_{UE-1}$ is calculated as

$$\begin{aligned}\mathcal{OP}_{UE_1} =&1-\Pr\left(|h_1|^2>\bar{\theta}\left(\Delta|g_1|^2+1\right)\right)\\ =&1-\int_0^{\infty} f_{|g_1|^2}(x)\int_{\bar{\theta}(\Delta x+1)}^{\infty} f_{|h_1|^2}(y)\,dxdy\\ =&1-\sum_{q=0}^{\infty}\sum_{b=0}^{\infty}\frac{K_{g_1}^b K_{h_1}^q \Lambda_{g_1}^{b+1}\Lambda_{h_1}^{q+1} e^{-\left(K_{h_1}+K_{g_1}\right)}}{b!q!\Gamma(b+1)\Gamma(q+1)}\\ &\times\int_0^{\infty} x^b e^{-\frac{(1+K_{g_1})}{\Omega_{g_1}}x}\int_{\bar{\theta}(\Delta x+1)}^{\infty} y^q e^{-\frac{\left(1+K_{h_1}\right)}{\Omega_{h_1}}y}dxdy,\end{aligned} \tag{13}$$

where $\Lambda_{g_1}=\frac{(1+K_{g_1})}{\Omega_{g_1}}$, $\Lambda_{h_1}=\frac{(1+K_{h_1})}{\Omega_{h_1}}$ and $\Gamma(\cdot)$ is the Gamma function [23, Eq. (8.310)].

With the help of [23, Eq. (3.324.1)], [23, Eq. (1.111)], [23, Eq. (3.324.3)] we can further simplify the above as

$$\mathcal{OP}_{UE_1}=1-\sum_{q=0}^{\infty}\sum_{b=0}^{\infty}\sum_{j=0}^{q}\sum_{p=0}^{j}\binom{j}{p}\frac{q!\,(b+p)!\Delta^p\bar{\theta}^j K_{g_1}^b K_{h_1}^q \Lambda_{g_1}^{b+1}\Lambda_{h_1}^{j}}{b!q!j!\Gamma(b+1)\Gamma(q+1)\left(\Lambda_{g_1}+\Lambda_{h_1}\right)^{b+p+1}}e^{-\frac{\Omega_{h_1}\left(K_{h_1}+K_{g_1}\right)+\bar{\theta}\left(1+K_{h_1}\right)}{\Omega_{h_1}}}. \tag{14}$$

Case 2: $\kappa=0$, the outage probability without interference link of UE-1 is given by

$$\begin{aligned}\mathcal{OP}_{UE-1} =&1-\Pr\left(|h_1|^2>\bar{\theta}\right)\\ =&F_{|h_1|^2}\left(\bar{\theta}\right)\\ =&1-\mathcal{Q}\left(\sqrt{2K_{h_1}},\sqrt{\frac{2(1+K_{h_1})\bar{\theta}}{\Omega_{h_1}}}\right).\end{aligned} \tag{15}$$

In particular, the outage probability with impact of interference at UE-2 is given by

$$\begin{aligned}\mathcal{OP}_{UE-2} =&1-\Pr\left(\Gamma_R^{s_2}>\varepsilon_2\cap\Gamma_R^{s_1}>\bar{\varepsilon}_1\right)\times\Pr\left(\Gamma_{UE-2}^{\tilde{s}_2}>\bar{\varepsilon}_2\right)\\ =&1-\underbrace{\Pr\left(|h_0|^2>\tilde{\theta}\left(\rho\kappa|g_0|^2+1\right)\right)}_{\phi_1}\times\underbrace{\Pr\left(|h_2|^2>\frac{\varepsilon_2}{\rho P L_2 d_2^{-\alpha}}\right)}_{\phi_2},\end{aligned} \tag{16}$$

where $\tilde{\theta}=\max\left(\frac{\varepsilon_2}{\rho d_S^{-\alpha}(\varphi_2-\varepsilon_2\varphi_1)},\frac{\bar{\varepsilon}_1}{\varphi_1\rho d_S^{-\alpha}}\right)$. Similarly with solving (13), it can be achieved $\phi_1$ as

$$\phi_1=\sum_{r=0}^{\infty}\sum_{a=0}^{\infty}\sum_{q=0}^{r}\sum_{w=0}^{q}\binom{q}{w}\frac{(a+w)!\rho^w\kappa^w\tilde{\theta}^q K_{g_0}^a K_{h_0}^r \Lambda_{g_0}^{a+1}\Lambda_{h_0}^{q}}{a!q!\Gamma(a+1)\Gamma(r+1)\left(\Lambda_{g_0}+\Lambda_{h_0}\right)^{a+w+1}}e^{-\frac{\Omega_{h_0}\left(K_{h_0}+K_{g_0}\right)+\tilde{\theta}\left(1+K_{h_0}\right)}{\Omega_{h_0}}}, \tag{17}$$

where $\Lambda_{g_0}=\frac{(1+K_{g_0})}{\Omega_{g_0}}$ and $\Lambda_{h_0}=\frac{(1+K_{h_0})}{\Omega_{h_0}}$. Next, $\phi_2$ is calculated as

$$\begin{aligned}\phi_2 =&\Pr\left(|h_2|^2>\frac{\varepsilon_2}{\rho P L_2 d_2^{-\alpha}}\right)\\ =&\int_{\frac{\varepsilon_2}{\rho P L_2 d_2^{-\alpha}}}^{\infty} f_{|h_2|^2}(x)\,dx\\ =&\sum_{c=0}^{\infty}\frac{K_{h_2}^c\Lambda_{h_2}^c(1+K_{h_2})e^{-K_{h_2}}}{c!\Gamma(c+1)\Omega_{h_2}}\int_{\frac{\varepsilon_2}{\rho P L_2 d_2^{-\alpha}}}^{\infty} x^c e^{-\Lambda_{h_2}x}dx,\end{aligned} \tag{18}$$

where $\Lambda_{h_2} = \frac{(1+K_{h_2})}{\Omega_{h_2}}$. Based on [[23], Eq. (3.351.2)], $\phi_2$ is given by

$$\phi_2 = \sum_{c=0}^{\infty} \frac{K_{h_2}^c \Lambda_{h_2}^c \left(1+K_{h_2}\right) e^{-K_{h_2}}}{c!\Gamma\left(c+1\right)\Omega_{h_2}\Lambda_{h_2}^{c+1}} \Gamma\left(c+1, \frac{\Lambda_{h_2}\varepsilon_2}{\rho P L_2 d_2^{-\alpha}}\right), \tag{19}$$

where $\Gamma\left(.,.\right)$ is the upper incomplete Gamma function [[23], Eq. (8.350.2)]. Substituting (18) and (16) into (15), $\mathcal{OP}_{UE-2}$ is given by

$$\begin{aligned}\mathcal{OP}_{UE-2} =& 1 - \sum_{r=0}^{\infty}\sum_{a=0}^{\infty}\sum_{q=0}^{r}\sum_{w=0}^{q}\sum_{c=0}^{\infty} \binom{q}{w} \frac{(a+w)!\rho^w \kappa^w \tilde{\theta}^q K_{g_0}^a K_{h_0}^r \Lambda_{g_0}^{a+1}\Lambda_{h_0}^q}{a!q!\Gamma\left(a+1\right)\Gamma\left(r+1\right)\left(\Lambda_{g_0}+\Lambda_{h_0}\right)^{a+w+1}} \\ &\times \frac{K_{h_2}^c \Lambda_{h_2}^c \left(1+K_{h_2}\right) e^{-K_{h_2}}}{c!\Gamma\left(c+1\right)\Omega_{h_2}\Lambda_{h_2}^{c+1}} \Gamma\left(c+1, \frac{\Lambda_{h_2}\varepsilon_2}{\rho P L_2 d_2^{-\alpha}}\right) e^{-\frac{\Omega_{h_0}\left(K_{h_0}+K_{g_0}\right)+\bar{\theta}\left(1+K_{h_0}\right)}{\Omega_{h_0}}}.\end{aligned} \tag{20}$$

## 4. NUMERICAL RESULTS

To perform simulations, we set $K = K_{h_0} = K_{h_1} = K_{h_2} = K_{g_0} = K_{g_1} = 2$ and $\Omega = \Omega_{h_0} = \Omega_{h_1} = \Omega_{h_2} = \Omega_{g_0} = \Omega_{g_1} = 1$; power allocation factors are $\varphi_1 = 0.2$ and $\varphi_2 = 0.8$; target rates are $R_1 = 1$ and $R_2 = 0.5$; coefficient related to SI from FD is $\kappa = 0.01$. Path loss exponent is $\alpha = 2$, the height of UAV $H = 30m$, additional attenuation factor is $\upsilon = 20$ (dB), environment parameter is $p = 4.8860$, environment parameter is $q = 0.4290$. The times of Monte Carlo simulation $10^6$, $\bar{d}_1 = 0.7$. In Figure 2, outage performance of user UE-2 is better than that of UE-1 at numerous case of Rician fading parameters. It is valuable as well-matching between Monte-Carlo and analytical simulations. At higher SNR, improved outage performance can be seen. As illustration in Figure 3, it is existence of optimal outage performance of user UE-1 as varying $a_2$ from 0.5 to 1. It can be further seen that lower SI leads to better outage performance at two users. While Figure 4 indicates that improvement outage performance happens at higher value of $K$ related to Rician fading channel.

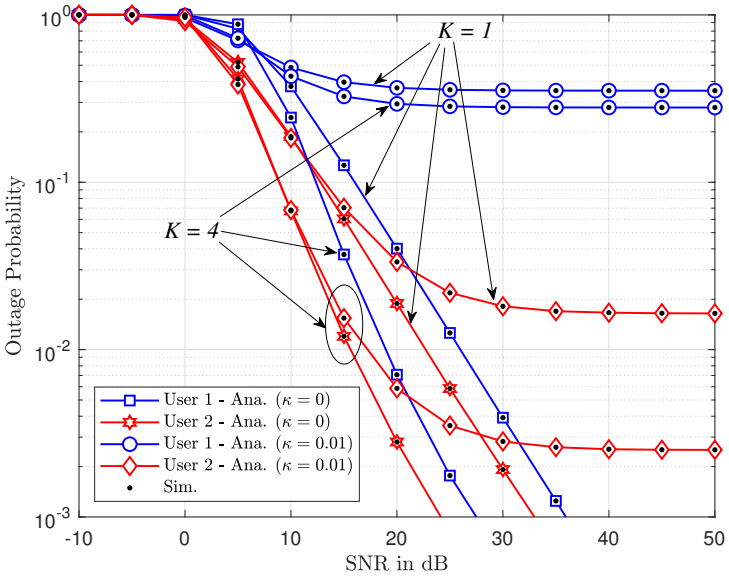


Figure 2. Outage probability versus SNR

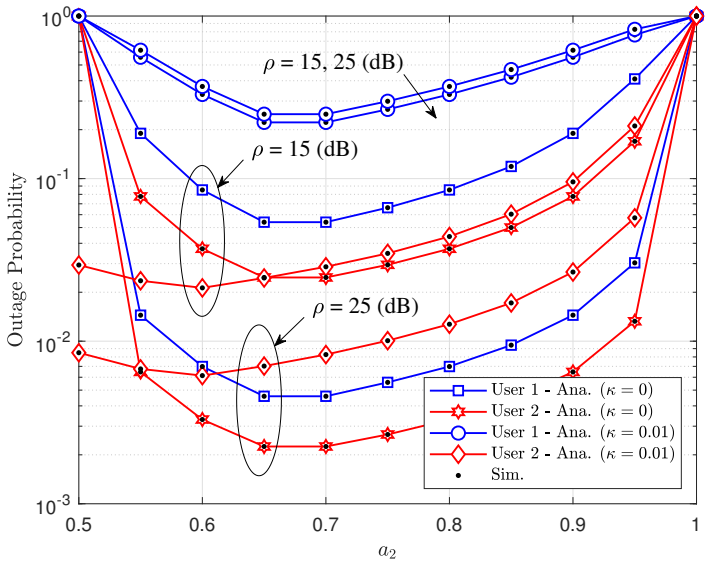


Figure 3. Impact of power allocation factor $a_1$ on outage performance, with $K = 2$

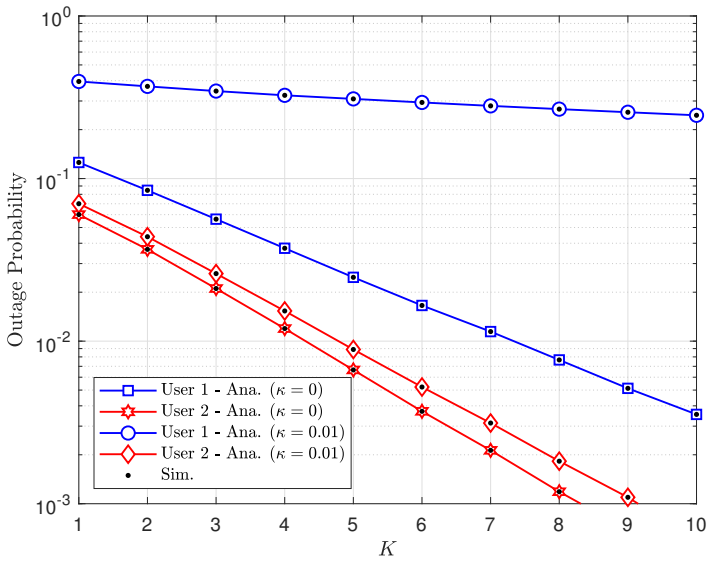


Figure 4. Impact of $K$ on outage performance, with $\rho = 15$ (dB)

## 5. CONCLUSION

In this paper, we have discussed how impacts of Rician fading and full-duplex mode have been implemented in the relaying network. We have explored several exact expressions of outage probability to show performance of each user. This findings benefit to deployment of full-duplex to provide higher spectrum efficiency for cellular network in practice.

## REFERENCES

[1] S. M. R. Islam, N. Avazov, O. A. Dobre, and K. S. Kwak,"Power-domain non-orthogonal multiple access (NOMA) in 5G systems: Potentials and challenges," *IEEE Commun. Surveys Tuts.*, vol. 19, no. 2, pp. 721-742, 2017.

[2] P. M. Nam, D. T. Do, T. T. Nguyen, P. T. Tin, "Energy harvesting assisted cognitive radio: random location-based transceivers scheme and performance analysis," *Telecommunication Systems*, vol. 67, no. 1, pp. 123-132, 2018.

[3] D. T. Do and A. T. Le, "NOMA based cognitive relaying: Transceiver hardware impairments, relay selection policies and outage performance comparison," *Computer Communications*, vol. 146, pp. 144-154, 2019.
[4] D. T. Do, M. Vaezi and T. L. Nguyen, "Wireless Powered Cooperative Relaying using NOMA with Imperfect CSI," in *Proc. of IEEE Globecom Workshops (GC Wkshps)*, Abu Dhabi, UAE, pp. 1-6, 2018.
[5] Dinh-Thuan Do and M. S. Van Nguyen, "Device-to-device transmission modes in NOMA network with and without Wireless Power Transfer," *Computer Communications*, vol. 139, pp. 67-77, May 2019.
[6] C. Zhong and Z. Zhang, "Non-orthogonal multiple access with cooperative full-duplex relaying," *IEEE Commun. Lett.*, vol. 20, no. 12, pp. 2478-2481, 2016.
[7] J. B. Kim and I. H. Lee, "Non-orthogonal multiple access in coordinated direct and relay transmission," *IEEE Commun. Lett.*, vol. 19, no. 11, pp. 2037-2040, 2015.
[8] W. Duan, M. Wen, Z. Xiong, and M. H. Lee, "Two-stage power allocation for dual-hop relaying systems with non-orthogonal multiple access," *IEEE Access*, vol. 5, pp. 2254-2261, 2017.
[9] Z. Ding, M. Peng, and H. V. Poor, "Cooperative non-orthogonal multiple access in 5G systems," *IEEE Commun. Lett.*, vol. 19, no. 8, pp. 1462-1465, 2015.
[10] R. Sun, Y. Wang, X. Wang, and Y. Zhang, "Transceiver design for cooperative non-orthogonal multiple access systems with wireless energy transfer," *IET Commun.*, vol. 10, no. 15, pp. 1947-1955, 2016.
[11] D. Niyato and E. Hossain, "A game-theoretic approach to competitive spectrum sharing in cognitive radio networks," *Proc. IEEE Wireless Commun. Netw. Conf.*, pp. 16-20, 2007.
[12] Z. Zhang, Z. Ma, M. Xiao, Z. Ding, and P. Fan, "Full-duplex device-to-device aided cooperative non-orthogonal multiple access," *IEEE Trans. Veh. Technol.*, vol. 66, no. 5, pp. 4467-4471, 2017.
[13] Z. Wei, X. Zhu, S. Sun, J. Wang, and L. Hanzo, "Energy-efficient full-duplex cooperative non-orthogonal multiple access," *IEEE Trans. Veh. Technol.*, vol. 67, no. 10, pp. 10123-10128, 2018.
[14] D-T. Do et al. "Wireless power transfer enabled NOMA relay systems: two SIC modes and performance evaluation," *TELKOMNIKA Telecommunication Computing Electronics and Control*, vol. 17, no.6, pp. 2697-2703, 2019.
[15] Dinh-Thuan Do, Chi-Bao Le and A.-T. Le, "Cooperative underlay cognitive radio assisted NOMA: secondary network improvement and outage performance, " *TELKOMNIKA Telecommunication Computing Electronics and Control*, vol. 17, no. 5, pp. 2147-2154, 2019.
[16] Dinh-Thuan Do and T.-T. Thi Nguyen, "Exact Outage Performance Analysis of Amplify-and Forward-Aware Cooperative NOMA," *TELKOMNIKA Telecommunication Computing Electronics and Control*, vol. 16, no. 5, pp. 1966-1973, 2018.
[17] Dinh-Thuan Do and C.-B. Le, "Exploiting Outage Performance of Wireless Powered NOMA," *TELKOMNIKA Telecommunication Computing Electronics and Control*, vol. 16, no. 5, 1907-1917.
[18] T. L. Nguyen and Dinh-Thuan Do, "Exploiting Impacts of Intercell Interference on SWIPT-assisted Non-orthogonal Multiple Access," *Wireless Communications and Mobile Computing*, vol. 2018, no. 17, 2018.
[19] D. T. Do, M.-S. V. Nguyen, "Outage probability and ergodic capacity analysis of uplink NOMA cellular network with and without interference from D2D pair," *Physical Communication*, vol. 37, 2019.
[20] Dinh-Thuan Do, A. Le and B. M. Lee, "NOMA in Cooperative Underlay Cognitive Radio Networks Under Imperfect SIC," *IEEE Access*, vol. 8, pp. 86180-86195, 2020.
[21] D. T. Do, A. T. Le and B. M. Lee, "On Performance Analysis of Underlay Cognitive Radio-Aware Hybrid OMA/NOMA Networks with Imperfect CSI," *Electronics*, vol. 8, no. 7, pp. 819-839, 2019.
[22] D. T. Do, A. T. Le, C. B. Le and B. M. Lee, "On Exact Outage and Throughput Performance of Cognitive Radio based Non-Orthogonal Multiple Access Networks With and Without D2D Link," *Sensors*, vol. 19 no. 15, pp. 3314-3330, 2019.
[23] I. S. Gradshteyn and I. M. Ryzhik, *Table of Integrals, Series and Products*, 6th ed. New York, NY, *USA: Academic Press*, 2000.
[24] Aitong Han, Tiejun Lv and Xuewei Zhang, "Outage Performance of NOMA-based UAV-Assisted Communication with Imperfect SIC," *IEEE Wireless Communications and Networking Conference (WCNC)*, April 2019.
[25] P. K. Sharma and D. I. Kim, "UAV-Enabled Downlink Wireless System with Non-Orthogonal Multiple Access," *IEEE Globecom Workshops (GC Wkshps)*, Singapore, pp. 1-6, 2017.